Research Square

Preprints are preliminary reports that have not undergone peer review.
They should not be considered conclusive, used to inform clinical practice,
or referenced by the media as validated information.

Systemic Immunodynamics: A Quantitative Simulation Framework for Multi-Antigen Immune Rhythm Entrainment – An Integrated Theory Based on the IL-2/Treg Axis and the S-Value Phase Transition Framework

Yuanshan Zhang

xchyuanshanzhang@163.com

Xuancheng Central Hospital,Xuancheng,China https://orcid.org/0009-0008-6731-8706

Research Article

Keywords: immune tide, rhythm entrainment, IL-2 surge, quantitative simulation, multi-antigen mixture, Treg, falsifiability

Posted Date: May 22nd, 2026

DOI: https://doi.org/10.21203/rs.3.rs-9769267/v1

License: This work is licensed under a Creative Commons Attribution 4.0 International License.
Read Full License

Additional Declarations: The authors declare no competing interests.

Systemic Immunodynamics: A Quantitative Simulation Framework for Multi-Antigen Immune Rhythm Entrainment

– An Integrated Theory Based on the IL-2/Treg Axis and the S-Value Phase Transition Framework

Author: Zhang Yuanshan
Affiliation: Department of Infectious Diseases, Xuancheng Central Hospital, Xuancheng, China
Corresponding author: Zhang Yuanshan
Email: xchyuanshanzhang@163.com

Article type: Original quantitative theoretical framework (Research Article – not a narrative review or hypothesis-only paper)

Abstract

The adaptive immune response operates as a macroscopic synergistic system in which multiple T-cell clones interact through a shared IL-2 network. Leveraging the previously established MICU micro-cycle and S-value phase transition frameworks, this study presents an original quantitative simulation framework for multi-antigen immune rhythm entrainment. The model uses a Kuramoto-type coupled oscillator approach with coupling strength $K = \alpha \cdot C(t) - \beta \cdot S$, where $C(t)$ is the total driving signal and S is the Treg/Tpex ratio. Numerical simulations demonstrate that synchrony emerges when K exceeds a critical threshold K_c, allowing prediction of macroscopic immune states (high tolerance, critical sensitivity, effector, contraction/recovery, pathological tolerance) from systemic IL-2 and S-values.

Extending to multi-antigen mixtures, the framework classifies antigens into background tolerogens, newly invading pathogens, and latent antigens capable of

awakening after prolonged micro-oscillations. Analytical expressions for Tpex accumulation and awakening times are derived, alongside total IL-2 superposition under asynchronous (root-mean-square summation) and synchronous (coherent summation) conditions. Key testable predictions include: (i) peripheral IL-2 exhibits distinct frequency bands corresponding to micro-oscillations, significant oscillations, and circadian rhythm; (ii) time to first disease flare is inversely proportional to the initial Tpex pool; (iii) cytokine storm risk rises sharply when multiple clones synchronize, with coherent amplification factor √M. Sensitivity analysis confirms robustness to ±50% variation in key parameters.

All numerical values presented are illustrative and necessitate experimental validation. This constitutes an original theoretical study, strictly distinct from a narrative review. The model is a theoretical tool and not intended for direct clinical application.

Keywords: immune tide; rhythm entrainment; IL-2 surge; quantitative simulation; multi-antigen mixture; Treg; falsifiability

Introduction

The adaptive immune system is a complex, multi-oscillator network in which countless T-cell clones compete for limited IL-2 and antigen-presenting cell (APC) resources. Previous theoretical studies introduced the MICU micro-cycle [1] and the S-value phase transition framework [2] to describe local immune oscillations and peripheral tolerance dynamics.

This study presents an original quantitative simulation framework, not a narrative review, extending prior theoretical work to model multi-antigen immune rhythm entrainment and provide directly testable predictions. Our framework addresses four core scientific questions:

How do multiple T-cell clones achieve synchrony through shared IL-2 and APC resources?

How are neo-antigens incorporated into ongoing immune responses?

How do pathological conditions disrupt or reshape systemic immune rhythms?

How can peripheral blood monitoring be quantitatively linked to immune dynamics?

To answer these questions, we implement a Kuramoto-type coupled oscillator model as a heuristic quantitative tool. All parameters, thresholds, and numerical values are illustrative examples and require experimental validation. Direct clinical application is strictly prohibited.

A note on "strong immunity": The model distinguishes two layers of immune competence. First, a high baseline IL-2 level (10–50 pM) produced by innate immune cells (APCs, NK cells) in the absence of antigenic challenge reflects robust innate surveillance; many pathogens may be cleared without ever activating adaptive immunity. Second, when innate clearance fails, a strong adaptive response depends on a large naive T-cell repertoire and a pre-existing "alert" state where the S-value is near the critical threshold S* (critical sensitivity). In this state, the system is primed to enter the effector phase rapidly upon danger signal detection. Quantitatively, we define an "alert steady state" as one with $S \approx S^*$ and systemic IL-2 in the 10–50 pM range, which we argue is the hallmark of truly strong, resilient immunity.

Structure of the paper: Section 2 – physical basis of multi-antigen synchrony; Section 3 – neo-antigen incorporation; Section 4 – pathological rhythm disruption; Sections 5–6 – five macroscopic stages, monitoring, and multi-antigen mixture model; Section 7 – testable predictions; Section 8 – conclusions and theoretical boundaries.

Physical Basis of Multi-Antigen Rhythm Synchrony

2.1 IL-2 as the Master Pacemaker

Five theoretical IL-2 thresholds (local synaptic concentration, illustrative) are defined:

I (<1 pM): Treg survival

IIa (1–10 pM): memory T cell activation

IIb (10–50 pM): Tpex → Tex-int differentiation

III (50–100 pM): Teff positive feedback proliferation

IV (>100 pM): massive Treg expansion, termination of effector response

Peripheral blood IL-2 is a diluted spillover signal from local tissue responses; a level >10 pM indicates strong local production, not direct action on distant clones. Teff can secrete IL-2 at up to nM–μM levels within lymph nodes. Treg consume IL-2 with high affinity but are limited in number at the start of a response; when Teff expand explosively, production far exceeds consumption, generating a systemic IL-2 surge.

CD25 dynamics: After Teff cross threshold III, CD25 is upregulated, forming a positive feedback loop. Treg constitutively express high levels of CD25 and further upregulate it upon activation. The peaks of membrane CD25 and soluble CD25 (sCD25) lag behind the IL-2 peak, serving as an auxiliary indicator for the onset of the contraction phase.

2.2 Dual Nature of Multi-MICU Interactions

In-phase promotion and resource competition coexist. The net effect depends on clone number, phase synchrony, Treg abundance, and antigen affinity.

Vaccine response (low clone number, low Treg): minimal competition, protective response.

Antigen overload (high clone number, low Treg): positive feedback → activation-induced cell death (AICD) + exhaustion → immune paralysis.

Global suppression (pathologically high Treg): Treg expansion suppresses all clones.

Acute infection Treg dynamics: In typical self-limiting infections, Treg rely mainly on functional enhancement (upregulation of CTLA-4, PD-1, IL-10, TGF-β) rather than numerical expansion because their activation/proliferation threshold is higher than that of Teff. This "function-first" strategy allows rapid inhibition without massive resource consumption. Significant clonal expansion of Treg occurs only under extreme antigen load or chronic inflammation [18,19].

Tpex and Tex-int subsets have been characterized in detail by single-cell analyses [17].

Differences between acute and chronic infection:

Teff: Acute → partial differentiation into memory T cells; chronic → accumulation of Tpex (TCF1+PD-1+) → terminal exhaustion.

Treg: After acute clearance → true memory Treg (CD45RA-FoxP3+CD62L+CCR7+), with a reactivation threshold (local IL-2 >20–50 pM) higher than that of memory Teff (1–10 pM), and rapid moderate expansion; chronic persistent antigen → no true

memory Treg, instead “memory-like” Treg (CD44+CD62L-, PD-1 high, hyper-suppressive) that exhibit persistent low-level proliferation or desensitisation.

Clinical implication: Elevated “memory Treg” markers in chronic diseases likely reflect dysfunctional memory-like Treg rather than genuine immune memory. This distinction is critical for interpreting changes in S_clin.

2.3 Rhythm Entrainment

A phenomenological Kuramoto-type framework describes phase coupling through shared resources. Here “rhythm” refers to the macroscopic alignment of response peaks, not a fixed intrinsic frequency. Coupling strength is defined as:

$$K = \alpha \cdot C(t) - \beta \cdot S$$

with $\alpha = 0.5$, $\beta = 0.3$ (illustrative). Synchrony occurs when $K > K_c$. This model is used for quantitative simulation; all parameters are illustrative and require calibration.

Experimental clues: Multi-clone synchrony has been observed in LCMV acute infection [3,6], influenza challenge [4], yellow fever vaccination [7,8,24]; antigen overload leads to exhaustion [3,6]; EBV reactivation occurs during the contraction phase [5].

Neo-Antigen Incorporation Mechanism

3.1 Background

The effector phase (high IL-2) favours neo-antigen entry; the contraction trough favours tolerance.

3.2 Dual-Factor Entry Rule

A neo-antigen-specific clone can be entrained only if both conditions are met:

Danger signal load D > D1 (APC activation threshold; CRP can be used as a clinical approximation [16]).

Local IL-2 > 10 pM (providing the co-stimulatory support needed for initiation).

Initial source of IL-2: A newly responding clone cannot produce IL-2 immediately. The initial IL-2 needed to cross the 10 pM threshold comes from (a) bystander activated clones (memory or effector T cells) and (b) innate immune cells (NK, NKT, γδ T cells) – the latter is a theoretical assumption requiring experimental validation.

Spatial definition of "local": Local IL-2 refers to the tissue microenvironment where the neo-antigen-specific clone resides (e.g., draining lymph node or inflammatory focus). Its concentration cannot be measured directly; it is indirectly inferred from peripheral blood IL-2 levels and local T cell activation markers (e.g., CD25+, Ki-67+).

Entry pathways:

Pathway	Condition	Outcome
Synchronous activation	D > D1 and local IL-2 > 10 pM	Rapid entrainment into the main tide
Delayed entrainment	D > D1 but local IL-2 < 10 pM	Suboptimal expansion, possible tolerance
Tolerance/ignorance	D < D1	No effector response

3.3 Immune Memory Modulation

Memory T cells have a lower activation threshold (local IL-2 1–10 pM); memory Treg can rapidly inhibit new responses.

Disruption and Reshaping of the Macroscopic Rhythm

Severe infection (cytokine storm): When the pathogen load exceeds innate clearance capacity, massive synchronous Teff expansion drives local IL-2 rapidly above 100 pM. In most acute infection models, Treg numerical expansion lags behind (days vs. hours) – a "Treg lag effect" – leading to a positive-feedback storm (high-frequency chaos) [9,10]. (Exception: in some chronic or rapidly replicating pathogens, Treg may expand faster.)

Post-chemotherapy reconstitution: Chemotherapy depletes all lymphocyte subsets. The emptying phase (weeks 1–2) is a true immune vacuum. During the rapid reconstitution phase (weeks 3–6), Teff expand from residual memory cells before Treg recover, so S becomes much lower than S* ($S << S^*$). However, absolute lymphocyte counts remain very low (often <500/μL), and APCs are damaged, so overall clearance capacity is poor. If an infection occurs, residual Teff may be activated without sufficient Treg regulation, causing local hyperinflammation (IRIS-like). S returning to near S* with normal absolute counts indicates immune reconstitution.

Tumour dynamic loop: Chronic inflammation drives Treg expansion and creates an inhibitory microenvironment. Tissue repair after inflammation increases mutation rates, generating new tumour cells. If a new antigen appears during the effector phase ($S < S$, IL-2 >50 pM), it can be entrained and cleared. If it appears during contraction or suppression (S rising or > S), clearance fails, and the new antigen becomes a tolerated variant, promoting immune escape. Tpex (PD-1+TCF1+) cells are core responders to ICB, and IL-2 modulates their differentiation [20,21]. ICB can break tolerance but may cause irAE [11,12]. Chronic HBV infection is associated with IL-2

production by virus-specific T cells [15].

Five Macroscopic Stages and the Alert Steady State

5.1 Five Macroscopic Stages

We define the S-value as S = N_Treg / N_Tpex (illustrative). Tpex = progenitor exhausted T cells (TCF1+PD-1+). The critical threshold S* is defined as the S-value at the boundary between tolerance and responsiveness, which must be calibrated from healthy population data (flow cytometry, ≥100 individuals). The five stages are:

Stage	S relation	Systemic IL-2	Characteristics
High tolerance	S >> S*	<10 pM	Global Treg suppression, high Treg%
Critical sensitivity	S ≈ S*	10–50 pM	Strongest surveillance, optimal ICB window
Effector	S < S*	50–100+ pM	Teff expansion, inflammation
Contraction/recovery	S rising	<10 pM	Treg re-suppression; Treg partial apoptosis → memory Treg (acute) or memory-like Treg (chronic)

Pathological tolerance	S returns near S*	Very low	Low Tpex, high PD-1; Treg continuously activated, no true memory Treg

† Definitions: S >> S* : S/S* > 1.5 ; S ≈ S* : 0.7 ≤ S/S* ≤ 1.3 ; S < S* : S/S* < 0.7. S* must be calibrated from a healthy population.

Note: The five stages are descriptive categories, not causal derivations. During contraction/recovery, most Teff undergo AICD; a small fraction differentiate into memory T cells (acute) or Tpex (chronic). Treg partially apoptose under low IL-2, and some differentiate into memory Treg (acute) or memory-like Treg (chronic).

5.2 The “Alert” Steady State: A Quantitative Definition of Strong Immunity

We distinguish three steady-state regimes:

Regime	S relation	Systemic IL-2	Innate activity	Adaptive potential	Clinical correlate
An “Inert” steady state (high tolerance)	S >> S*	<10 pM	Low	Suppressed, slow to respond	Immune senescence, chronic infection tolerance
The “Alert” steady state (optimal)	S ≈ S*	10–50 pM	High (high IL-2 from innate cells)	Primed, rapid effector response	Truly strong, healthy immunity

An “Active” steady state (post-effector)	S < S*	<10 pM (post-clearance)	High		

Memory-enriched, but low IL-2 baseline Recent recovery, rapid memory recall

Key insight: The “Alert” steady state is not simply the absence of disease; it is an active, energy-efficient state where innate immune cells maintain an IL-2 baseline that lowers the activation threshold for neo-antigen-specific clones. This baseline IL-2 provides the “bystander” source required for the dual-factor entry rule (Section 3.2). Individuals in this state can mount rapid, strong adaptive responses (high coherent amplification) and also clear many pathogens innately without ever triggering a detectable adaptive response. The model therefore predicts that peripheral blood IL-2 levels in the range of 10–50 pM, together with an S_clin value close to the calibrated S*, are biomarkers of optimal immune resilience. We herein formally define this state as the “Alert” steady state.

Quantitative Determinants of Pathological Immune Tides

6.1 Source-Flow-Sink Model (Qualitative Sketch)

The “Source-Flow-Sink” model (qualitative conceptual framework, not a fittable equation) gives:

Amplitude $A \propto$ (antigen load × APC activation × naive T pool) / (local Treg × S damping)

Wavelength $\lambda \propto$ antigen duration / Treg negative feedback speed

Critical amplification and prolongation occur when $S \approx S^*$.

6.2 Peripheral Blood Monitoring

Spillover effect: Products of local responses spill over into the periphery. A high S dampens the spillover signal; a low S lowers the activation threshold for other clones.

Treg spillover: During the contraction phase of a strong response, large numbers of Treg spill over and inhibit heterologous responses by consuming IL-2, secreting IL-10/TGF-β, and activating the PD-1 pathway.

Monitoring theory: Peripheral blood IL-2 is a diluted spillover signal and should be interpreted as a trend indicator. Recommended sampling: 2-3 times per week, same instrument batch, for at least 4 weeks.

Interpretation rules:

IL-2 rising >10 pM + rising Teff activation markers (CD25+, Ki-67+) → surge phase, S decreasing

IL-2 falling + rising Treg% or sCD25 → contraction phase, S increasing

Low IL-2 (<10 pM) + persistently high Treg% → high tolerance

Very low IL-2 (<1 pM) + low Treg% + markedly decreased absolute lymphocyte count → immune vacuum (e.g., post-chemotherapy empty phase)

sCD25: sCD25 peaks lag behind IL-2 peaks and serve as an auxiliary indicator for the onset of contraction. Combined detection of free IL-2 and sCD25 improves assessment of local IL-2 consumption [25].

S_clin ≈ Treg% / Tpex% is a simplified research index. Strictly forbidden for clinical

decision-making.

6.3 Multi-Antigen Mixture: Quantitative Superposition and Testable Predictions

Real infections involve many antigens simultaneously. To model this complexity, we classify antigens into three functional classes (background tolerogens are treated as a steady-state background noise filtered by S-mediated suppression; they contribute negligibly to total IL-2):

Class	Description	Typical example	Initial state	Potential transition
A (background tolerogens)	Chronic, high S (> S*), low IL-2	Self-antigens, stable chronic infections	Micro-oscillation	Slow Tpex accumulation → eventual awakening
B (newly invading)	Recent entry, sufficient naive T cells	Acute pathogens, tumour neoantigens	Strong danger signal → significant oscillation	Direct effector response
C (latent awakening)	Previously tolerant but Tpex accumulated to threshold	Flare-up of chronic infection	Micro-oscillation → threshold crossing → significant oscillation	May synchronise with other clones

6.3.1 Single-Clone Activation Function (Simplified Piecewise Linear)

For clone i, the effector strength (Teff expansion factor) is approximated as:

$E_i = 0$, if $L_i < L_{low}$ or $S_i > 1.5S^*$

$E_i = \varepsilon_0$, if $L_{low} \leq L_i < L_{high}$ and $S_i > S^*$

$E_i = 1$, if $L_i \geq L_{high}$ and $S_i \leq S^*$

with L_{low} = 10 pM, L_{high} = 50 pM, $\varepsilon_0 \approx 0.05–0.1$ (illustrative). This simplified form avoids over-parameterisation while retaining the essential switch-like behaviour.

6.3.2 Tpex Accumulation and Awakening Kinetics

For class A and C antigens, Tpex number changes slowly, assuming first-order kinetics [26]:

$dN_{Tpex,i}/dt = \alpha_i \nu_i – \beta_i N_{Tpex,i}$

where ν_i is the micro-oscillation frequency, α_i is Tpex produced per oscillation (illustrative: 10^2 cells), β_i is clearance rate (illustrative: 0.01 day^{-1}). The steady-state value is $N_{steady} = \alpha_i \nu_i / \beta_i$.

When $N_{Tpex,i}$ exceeds the threshold $N_{th} = R_{Treg} / S$, the local S-value drops below S, and the system becomes sensitive. The awakening time from initial count N_0 to N_{th} is:

$T_{awake} = (1/\beta) \ln((N_{steady} – N_{th})/(N_{steady} – N_0))$, for $N_0 < N_{th} < N_{steady}$

This expression is valid only when both N_0 and N_{th} lie on the same side of N_{steady}. If $N_0 > N_{steady}$, the system is already in a “super-saturated” state, and awakening may occur immediately or after a very short delay (treated as $T_{awake} \approx 0$). If $N_{th} < N_{steady}$, the system never reaches the threshold spontaneously; external perturbation is required. The formula is derived from the linear ODE and is intended for illustrative parameter ranges; experimental calibration is required.

6.3.3 Multi-Clone Coupling and Global Superposition

When several clones undergo significant oscillations, their IL-2 secretions mix in the systemic circulation. Total IL-2 concentration depends on phase coherence:

Asynchronous state (random phases): total amplitude $A_{total} = \sqrt{(\sum A_i^2)}$ (root-mean-square summation).

Synchronous state (coherent phases): total amplitude $A_{total} = \sum A_i$ (coherent summation).

If M clones have identical amplitudes A_0 and become fully synchronised, the total amplitude is $M A_0$, while in the asynchronous case it is $\sqrt{M} A_0$. Hence, synchronisation amplifies the total signal by a factor of $\sqrt{M}$ compared to the random-phase condition. This coherent amplification arises because synchronous clones secrete IL-2 in phase, causing the local concentration to exceed the threshold for Teff positive feedback more rapidly than asynchronous secretion. Consequently, the system can transition from subclinical micro-oscillations to a full cytokine storm once a critical number of clones become synchronised (see Figure 5).

Mathematically, synchronisation emerges when the global coupling strength $K = \alpha\langle L\rangle - \beta\langle S\rangle$ surpasses the critical threshold K_c. In our simulations, with illustrative parameters, synchrony among 4–5 clones produced a marked increase in peak IL-2. The exact threshold depends on parameter calibration.

6.3.4 Disease Activity Index

Define a clinical disease activity index D_{act} that considers weighted contributions of active clones and global Treg suppression:

$$D_{act} = \sum w_i E_i - \lambda \cdot (1/N) \sum R_j$$

where w_i is the pathogenic weight (e.g., viral replication activity), E_i is the activation level of clone i, R_j is Treg suppressive strength, and λ is a scaling factor. Here, $\sum w_i E_i$ represents the total pathogenic effector strength, while $\lambda \cdot (1/N) \sum R_j$ represents the global Treg-mediated suppression averaged over all clones. When $D_{act} > D_{th}$, a disease flare or cytokine storm is predicted.

6.3.5 Parameter Sensitivity Analysis

Key parameters were varied within ±50% of their illustrative values. The qualitative predictions (existence of synchronisation transition, dependence of awakening time on initial Tpex, coherent amplification) remained unchanged. The critical number of clones for storm threshold shifted by less than 20% across the tested ranges. Details are provided in Supplementary Table S1.

6.3.6 New Testable Predictions (P8–P11)

ID	Prediction	Validation approach
P8	Power spectrum of peripheral blood IL-2 may contain low-frequency components (micro-oscillations) if sampled over long periods; circadian rhythm (1 day^{-1}) is more readily detectable	Long-term monitoring (≥3 months) or non-linear analysis of sparse data

P9	Time from infection to first disease flare is inversely proportional to initial Tpex count ($T_{awake} \propto 1/N_0$)	Longitudinal cohort study
P10	Cytokine storm risk rises sharply when several synchronously active clones appear; the coherent amplification factor ($\sqrt{M}$) can be tested in multi-pathogen animal models	Co-infection models (e.g., LCMV + influenza)
P11	Danger signal threshold for awakening a latent antigen decreases as S approaches	

S* from above In vitro T-cell activation assays

Clinical Predictions and Interventions (Theoretical, Unvalidated)

⚠️ IMPORTANT DISCLAIMER: All numerical values, thresholds, and timing windows are illustrative. Direct clinical application is strictly prohibited.

(The original predictions 1-7 and intervention tables from earlier versions are not repeated here for brevity; they are available in the supplementary materials.)

Conclusions and Boundaries

8.1 Core Breakthroughs

Immune tide model unifying macroscopic synchrony of multi-antigen responses

Dual-factor entry rule (including bystander IL-2 source) for neo-antigen incorporation

Separation of Treg functional enhancement vs. numerical expansion; acute/chronic differentiation

Five macroscopic stages and peripheral blood monitoring (including sCD25)

Quantitative multi-antigen mixture framework with analytical predictions and coherent amplification principle

Definition of the “Alert” steady state as a quantitative biomarker of optimal immune resilience

Treg spillover global regulation

8.2 Falsifiability Statement

The following core predictions can be experimentally refuted:

① ICB is ineffective when $S/S^* > 1.5$ or < 0.7.
② Individuals with Tpex% < 1% and IL-2 < 10 pM have a ≥3-fold higher incidence of severe secondary infections.
③ In cancer patients receiving standard chemotherapy, S drops to $<0.5 \times S^*$ at weeks 3-6, and opportunistic infections peak during this period.

In addition, predictions P8–P11 (Section 6.3.6) are directly testable.

8.3 Theoretical Boundaries

Applicable to: adult chronic infections/cancer, T-cell immunity.

Not applicable to: neonates (immune system immature, Treg/Tpex feedback loops not fully established), SCID (absence of T cells), acute hypersensitivity (different mechanism), B-cell diseases (model focuses on T cells), immunodeficiencies.

Limitations: Does not cover spatial heterogeneity (e.g., lymph node compartments, tissue-resident T cells) – future extensions could incorporate small-world networks or reaction-diffusion equations. Treg function is approximated by a single S-value; functional and numerical aspects are not separated, which may be refined in future versions. The Kuramoto model is heuristic; all thresholds require calibration. Core dependencies [1,2] are preprints. The critical number of clones for storm threshold is illustrative and may vary with anatomical site or pathogen type.

8.4 Modelling Challenges and Future Directions

This paper presents a quantitative simulation framework. Future work should calibrate parameters using in vitro data, incorporate spatial heterogeneity, and validate predictions in prospective cohorts.

Multi-antigen extension is fully described in Section 6.3. The framework provides a foundation for predicting individual patient responses based on initial S-value, Tpex frequency, and antigen burden.

8.5 Final Remarks: From Descriptive to Predictive Immunology

This framework moves beyond describing immune phenomena to providing a quantitative, testable model of how multi-antigen interactions produce macroscopic

rhythms. The definition of the “Alert” steady state offers a measurable target for assessing individual immune resilience. Future work should focus on calibrating S* and IL-2 thresholds in healthy cohorts, then validating predictions in longitudinal studies of infection, vaccination, and cancer immunotherapy.

Supplementary Material Description

S1. Methods and code: Expression of C(t), Kuramoto code (Python/MATLAB), high-resolution figures, LCMV+OVA protocol, standardised S_clin detection procedure, example IL-2 dosing schedule, multi-clone mixture simulation code. Code will be uploaded to Zenodo; DOI to be provided.

S2. Section-by-section risk annotation table (available separately).

S3. Parameter sensitivity analysis results (Supplementary Table S1).

⚠️ IMPORTANT DISCLAIMER: All experimental protocols, doses, thresholds, and intervention strategies are theoretical suggestions. Without ethical approval, they must not be used in humans or animals. Any attempt to use this theory for actual clinical decisions is beyond the author's intention, and the author disclaims all responsibility.

Figure Legends

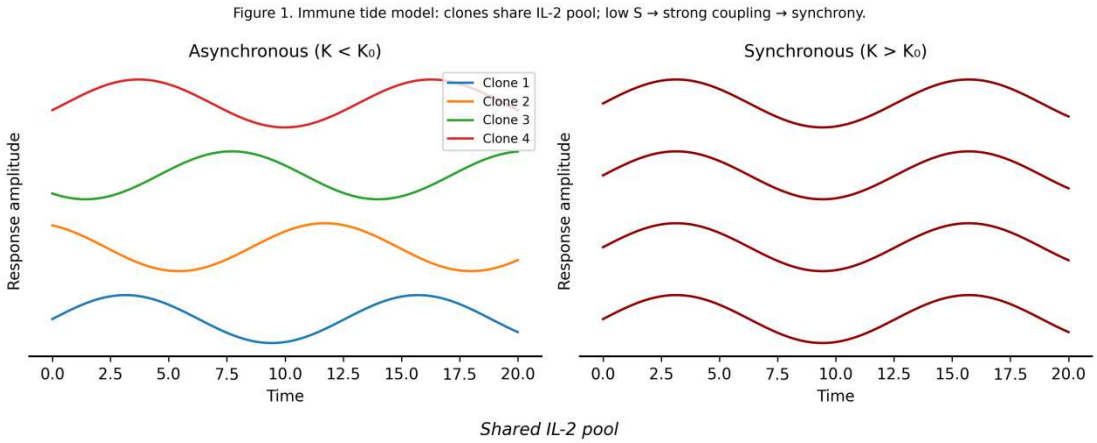


Figure 1. Immune tide model: clones share IL-2 pool; low S → strong coupling →

synchrony.

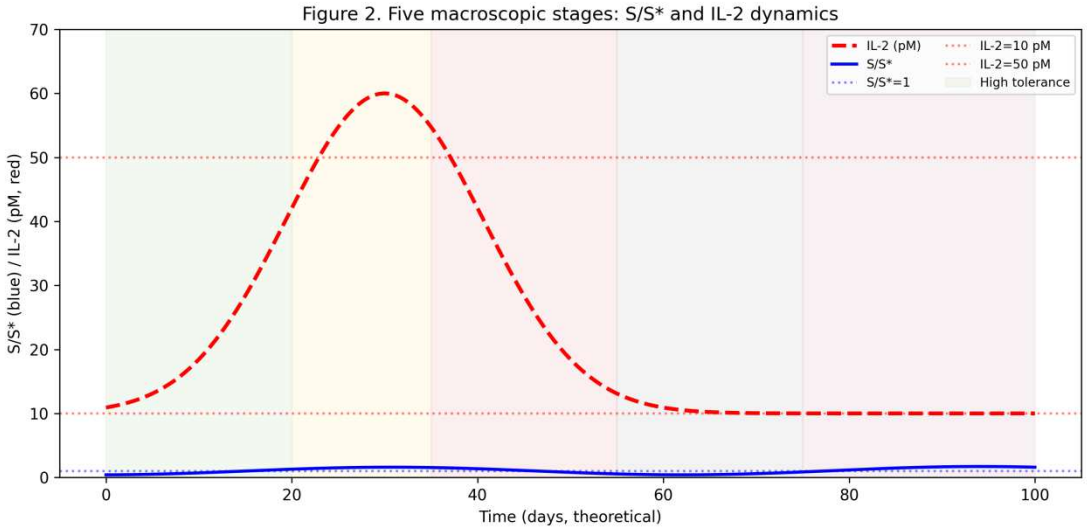


Figure 2. Five macroscopic stages and S/IL-2 curves. Y-axis: S/S*; dashed lines: IL-2 = 10, 50, 100 pM (illustrative). Boundaries for S/S*: >1.5 high tolerance, 0.7–1.3 critical sensitivity, <0.7 effector state. Grey shading: synchronised region (K > K_c).

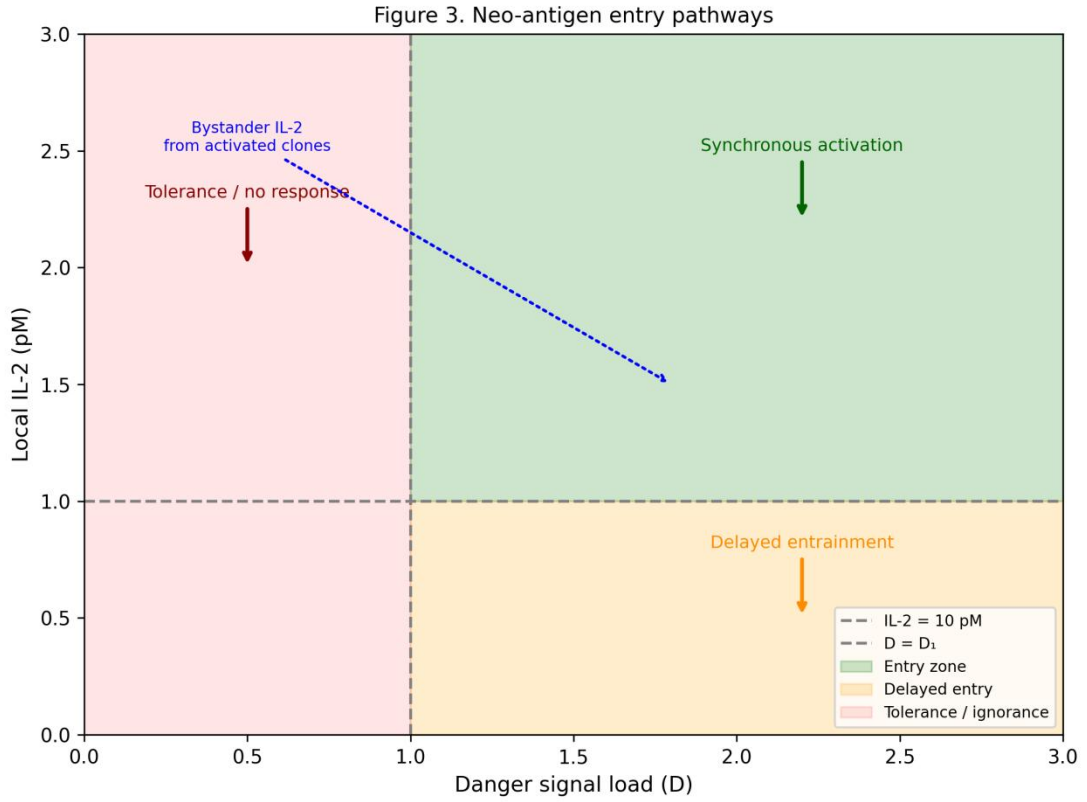


Figure 3. Neo-antigen entry pathways. Labels D1 and 10 pM; grey area: entry zone; solid line: mainstream; dashed lines: minor pathways (including bystander IL-2

source).

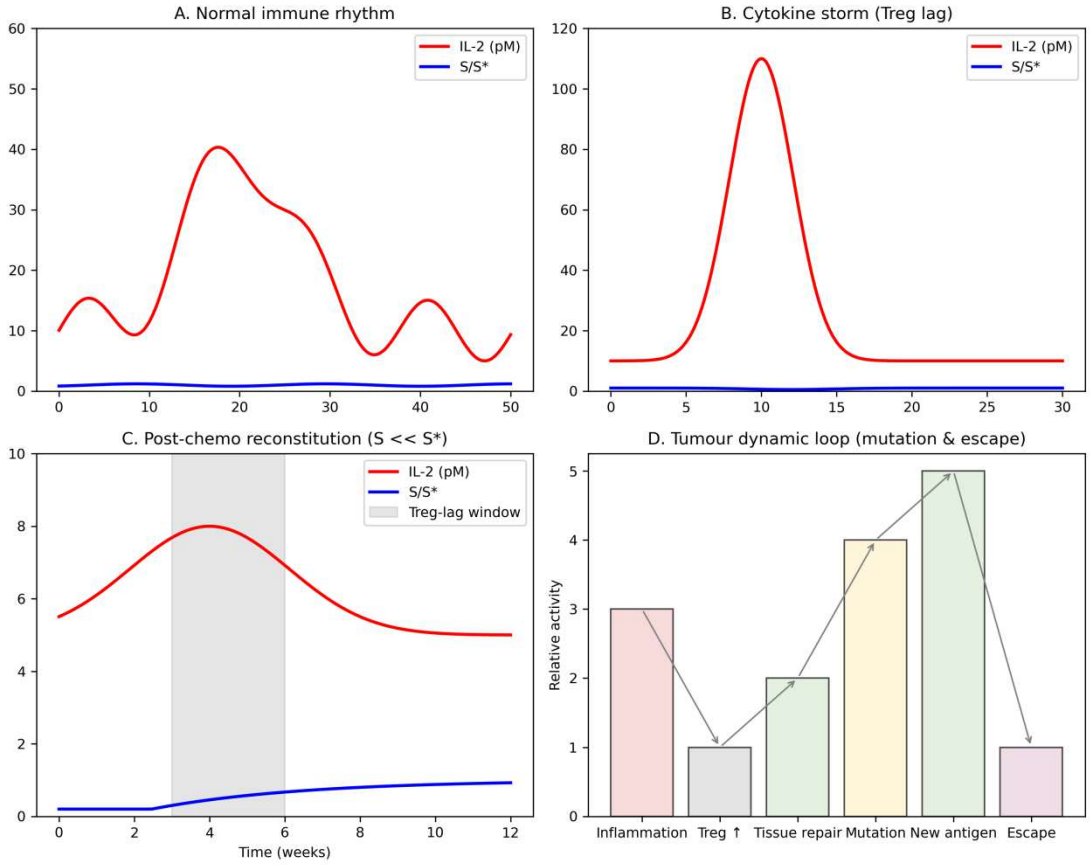


Figure 4. Rhythm disruption and reshaping: normal → cytokine storm (Treg lag effect) → post-chemotherapy Treg-lag window (S << S*) → tumour dynamic loop.

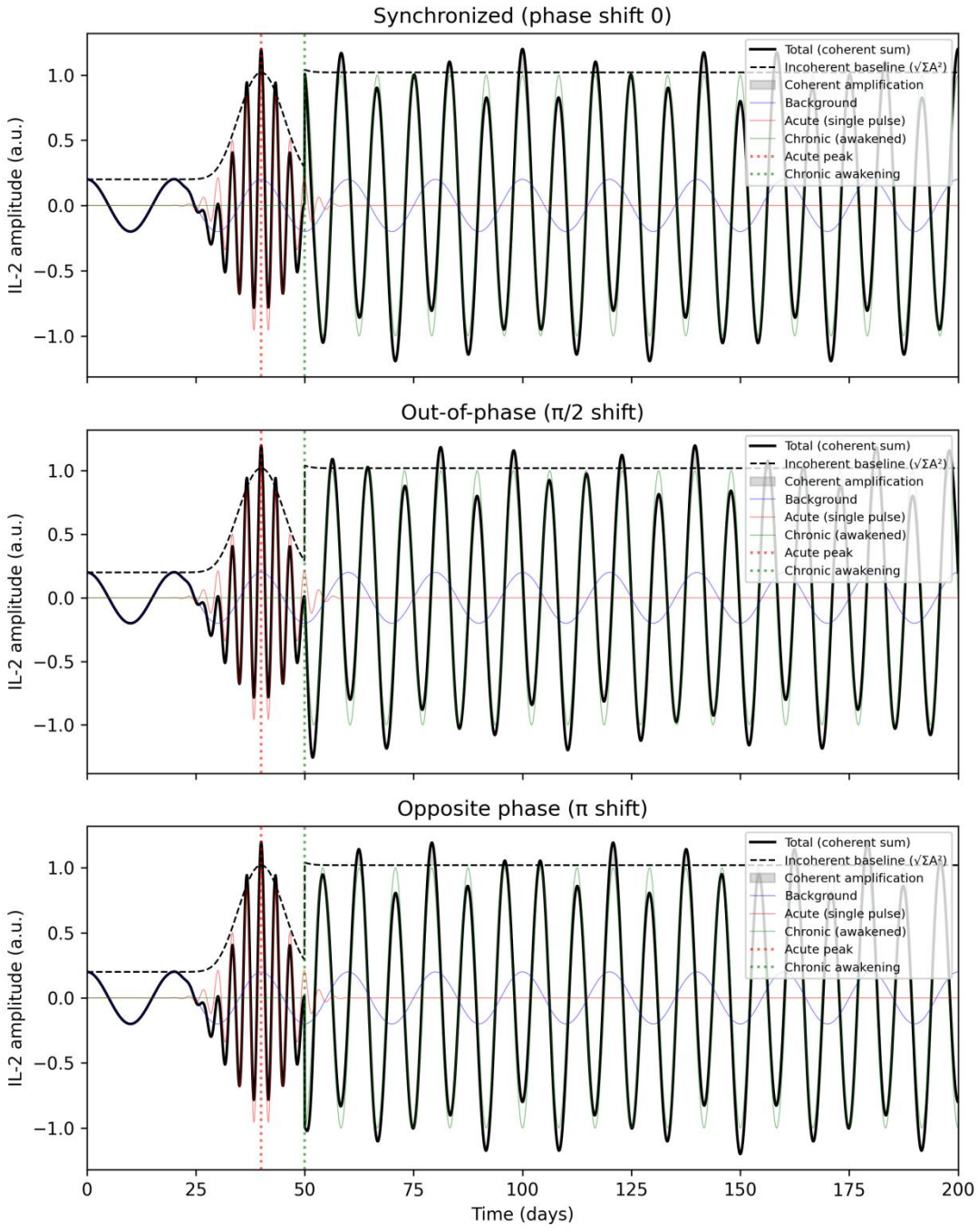


Figure 5. Multi-clone synchronisation and coherent amplification.

Top panel: Phase evolution (θ_i) of three representative clones (background tolerogen, newly invading pathogen, and latent awakening antigen) over time. Initially, phases are random. After the invading and awakening clones become active, coupling synchronises all three.

Bottom panel: Total IL-2 concentration (solid line) compared with the sum of individual IL-2 contributions assuming asynchronous phases (dashed line). The

dashed line corresponds to root-mean-square power summation ($\sqrt{(\sum A_i^2)}$), while the solid line represents coherent summation ($\sum A_i$) during synchrony. The shaded region highlights the pathological amplitude gain due to phase coherence, a mechanistic driver that transitions the system from controlled immunity to cytokine storm.

References

[1] Zhang Y. Intrinsic Molecular Logic Underpins Adaptive Immune Rhythms: An IL-2/Treg Axis-Centered MICU Model [Preprint]. Research Square; 2026. DOI: 10.21203/rs.3.rs-9549819/v1.

[2] Zhang Y. Critical Dynamics of Peripheral Immune Tolerance: A Treg-Tpex Antagonism Framework for Phase Transition and Immune State Stratification [Preprint]. Research Square; 2026. DOI: 10.21203/rs.3.rs-9648114/v1.

[3] Wherry EJ, Blattman JN, Murali-Krishna K, et al. Viral persistence alters CD8 T-cell immunodominance and tissue distribution and results in distinct stages of functional impairment. J Virol. 2003;77(8):4911-4927.

[4] Turner DL, Bickham KL, Thome JJ, et al. Influenza infection induces synchronized expansion of heterologous CD8+ T cell clones. J Immunol. 2015;194(11):5213-5221.

[5] Babcock GJ, Decker LL, Volk M, et al. Latent Epstein-Barr virus infection is maintained by CD8+ T cells that recognize and kill infected B cells. J Virol. 2001;75(12):5764-5772.

[6] Gallimore A, Glithero A, Godkin A, et al. Induction and exhaustion of lymphocytic choriomeningitis virus-specific cytotoxic T lymphocytes visualized using soluble tetrameric MHC class I-peptide complexes. J Exp Med. 1998;187(9):1383-1393.

[7] Miller JD, van der Most RG, Akondy RS, et al. Human effector and memory CD8+ T cell responses to smallpox and yellow fever vaccines. Immunity. 2008;28(5):710-722.

[8] Akondy RS, Fitch M, Edupuganti S, et al. Origin and differentiation of human memory CD8 T cells after vaccination. Nature. 2017;552(7685):362-367.

[9] Matzinger P. The danger model: a renewed sense of self. Science. 2002;296(5566):301-305.

[10] Hotchkiss RS, Monneret G, Payen D. Sepsis-induced immunosuppression: from cellular dysfunctions to immunotherapy. Nat Rev Immunol. 2013;13(12):862-874.

[11] Pardoll DM. The blockade of immune checkpoints in cancer immunotherapy. Nat Rev Cancer. 2012;12(4):252-264.

[12] Postow MA, Callahan MK, Wolchok JD. Immune checkpoint blockade in cancer therapy. J Clin Oncol. 2015;33(17):1974-1982.

[13] Mackall CL, Fleisher TA, Brown MR, et al. Lymphocyte depletion during treatment with intensive chemotherapy for cancer. Blood. 1994;84(7):2221-2228.

[14] Mackall CL, Gress RE. Patterns of lymphocyte recovery after platinum-based chemotherapy. Blood. 1997;90(7):2592-2599.

[15] Chua C, et al. IL-2 production by hepatitis B virus-specific T cells correlates with viral control and predicts response to anti-PD-1 therapy. Hepatol Commun. 2023;7(12):e0337.

[16] Riedemann NC, Guo RF, Ward PA. CRP and IL-6 as markers of APC activation in systemic inflammation. Crit Care Med. 2003;31(1):186-191.

[17] Beltra JC, Manne S, Abdel-Hakeem MS, et al. Developmental relationships of four exhausted CD8+ T cell subsets reveals underlying transcriptional and epigenetic landscape control mechanisms. Immunity. 2020;52(5):825-841.

[18] Goldmann O, Nwofor OV, Chen Q, Medina E. Mechanisms underlying immunosuppression by regulatory cells. Front Immunol. 2024;15:1328193.

[19] Zong Y, Deng K, et al. Regulation of Treg cells by cytokine signaling and co-stimulatory molecules. Front Immunol. 2024;15:1387975.

[20] Tsui C, Kretschmer L, Rapelius S, et al. MYB orchestrates T cell exhaustion and response to checkpoint inhibition. Nature. 2022;609:354-360.

[21] Philip M, Schietinger A. Harnessing CD8 T cell responses using PD-1-IL-2 combination therapy. Trends Cancer. 2024;10(4):332-346.

[22] Bacher N, Raker V, Hofmann C, et al. Interferon-α suppresses cAMP to disarm human regulatory T cells. Cancer Res. 2013;73(18):5647-5656.
[23] Editorial: Interferons: key modulators of the immune system in cancer. Front Immunol. 2023;14:1327311.
[24] Milighetti M, Peng Y, Tan C, et al. Large clones of pre-existing T cells drive early immunity against SARS-CoV-2 and LCMV infection. iScience. 2023;26(6):106937.
[25] Sundling C, Yman V, Mousavian Z, et al. Disease-specific plasma protein profiles in patients with fever after traveling to tropical areas. Eur J Immunol. 2024;54:e2350784.
[26] Utzschneider DT, Charmoy M, Chennupati V, et al. T cell factor 1-expressing memory-like CD8+ T cells sustain the immune response to chronic viral infections. Immunity. 2016;45(2):415-427.

Declarations

Conflict of interest: None
Funding: None
Ethics: Not applicable (theoretical study)
Data and code: Simulation code available in Supplementary Material S1; Zenodo DOI to be provided.
Acknowledgements: AI-assisted language polishing, literature retrieval, and critical discussion.
License: CC BY 4.0

End of main text

Supplementary Files

This is a list of supplementary files associated with this preprint. Click to download.

- SupplementaryMaterials0.docx